Video Article

Development and Characterization of *In Vitro* Microvessel Network and Quantitative Measurements of Endothelial $[Ca^{2+}]_i$ and Nitric Oxide Production

Sulei Xu*[1], Xiang Li*[1], Yuxin Liu[2], Pingnian He[1]

[1]Department of Cellular and Molecular Physiology, College of Medicine, Penn State University

[2]Lane Department of Computer Science and Electrical Engineering, West Virginia University

*These authors contributed equally

Correspondence to: Pingnian He at pinghe@hmc.psu.edu

URL: https://www.jove.com/video/54014
DOI: doi:10.3791/54014

Keywords: Cellular Biology, Issue 111, Microvessel, endothelial cell, intracellular calcium, nitric oxide, VE-cadherin, F-actin, microfluidics

Date Published: 5/19/2016

Citation: Xu, S., Li, X., Liu, Y., He, P. Development and Characterization of *In Vitro* Microvessel Network and Quantitative Measurements of Endothelial $[Ca^{2+}]_i$ and Nitric Oxide Production. *J. Vis. Exp.* (111), e54014, doi:10.3791/54014 (2016).

Abstract

Endothelial cells (ECs) lining the blood vessel walls *in vivo* are constantly exposed to flow, but cultured ECs are often grown under static conditions and exhibit a pro-inflammatory phenotype. Although the development of microfluidic devices has been embraced by engineers over two decades, their biological applications remain limited. A more physiologically relevant *in vitro* microvessel model validated by biological applications is important to advance the field and bridge the gaps between *in vivo* and *in vitro* studies. Here, we present detailed procedures for the development of cultured microvessel network using a microfluidic device with a long-term perfusion capability. We also demonstrate its applications for quantitative measurements of agonist-induced changes in EC $[Ca^{2+}]_i$ and nitric oxide (NO) production in real time using confocal and conventional fluorescence microscopy. The formed microvessel network with continuous perfusion showed well-developed junctions between ECs. VE-cadherin distribution was closer to that observed in intact microvessels than statically cultured EC monolayers. ATP-induced transient increases in EC $[Ca^{2+}]_i$ and NO production were quantitatively measured at individual cell levels, which validated the functionality of the cultured microvessels. This microfluidic device allows ECs to grow under a well-controlled, physiologically relevant flow, which makes the cell culture environment closer to *in vivo* than that in the conventional, static 2D cultures. The microchannel network design is highly versatile, and the fabrication process is simple and repeatable. The device can be easily integrated to the confocal or conventional microscopic system enabling high resolution imaging. Most importantly, because the cultured microvessel network can be formed by primary human ECs, this approach will serve as a useful tool to investigate how pathologically altered blood components from patient samples affect human ECs and provide insight into clinical issues. It also can be developed as a platform for drug screening.

Video Link

The video component of this article can be found at https://www.jove.com/video/54014/

Introduction

Endothelial cells (ECs) lining the blood vessel walls *in vivo* are constantly exposed to flow, but cultured ECs are often grown under static conditions and exhibit a pro-inflammatory phenotype[1,2]. The microfluidics technology enables a precisely controlled fluid through a geometrically constrained microscale (sub-millimeter) channels[3], which provides the opportunity for cultured cells, especially for vascular ECs, to grow under desired flow conditions. These features make the cell culture conditions closer to *in vivo* than the conventional, static 2D cell cultures. They are extremely important when the microfluidic devices are used to model different types of vasculatures and to study EC responses to mechanical and/or chemical stimulations.

Despite the advantages demonstrated by the microchannel network over a static cell culture, the adaptation and application of microfluidics in the biomedical field remain limited. Reported by a recent review, the majority of the publications of this field (85%) are still in engineering journals[4]. The performance of microfluidic devices has not been convincing enough for most biologists to switch from current techniques such as the Transwell assay and the macro-scale culture dish/glass slide to this miniaturized device. Microfluidics is a multidisciplinary field, which requires interdisciplinary collaborations to move this field forward. The objective of this technical article is to reduce the knowledge gaps between disciplines and make the fabrication procedures understandable by biologists, while providing biological application and functional validation of the microfluidic microvessels. The visualized experimental protocols include fabrication of both microfluidic devices and their biological utilities, which represents a close collaboration between engineers and biologists.

We recently reported some biological applications using the *in vitro* microvessel network with microfluidic device[5]. In order to appropriately design the dimensions of the microchannel network and apply the desired shear stress, a numerical model was built with computational fluid dynamic software to closely estimate the flow profile. Primary human umbilical vein endothelial cells (HUVECs) that were seeded into the microchannels reached confluence, *i.e.* covered the entire inner surfaces of the microchannel, in 3-4 days with continuous perfusion. The proper barrier formation was demonstrated by VE-cadherin staining and compared with those formed under static cell culture conditions and in intact

microvessels. By applying the experimental protocols developed in individually perfused intact microvessels[6-8], we quantitatively measured the changes in EC $[Ca^{2+}]_i$ and nitric oxide (NO) production in response to adenosine triphosphate (ATP) with fluorescent indicators and confocal and conventional fluorescence microscopy. The agonist-induced increases in EC $[Ca^{2+}]_i$ and NO production have been reported as necessary intracellular signals for inflammatory mediator-induced increases in microvessel permeability[6-15]. Although some previous studies showed images of DAF-2 DA loaded microfluidic devices[16,17], appropriate resolution and data analysis had not yet achieved[18]. To our knowledge, this study demonstrates the first quantitative measurements of agonist-induced dynamic change in endothelial $[Ca^{2+}]_i$ and NO production utilizing microfluidic based system.

Microfabrication techniques have the flexibility to fabricate microchannels down to a few microns and enable the development of complex patterns to mimic the geometries of *in vivo* microvasculature. Here we presented a typical microchannel network with three levels of branching. This network is fabricated by the combination of photolithography which is performed in a microfabrication cleanroom and soft lithography.

Protocol

1. Microfluidic Device Fabrication

1. Standard Photolithography Fabrication of a SU-8 50 Master Mold
    1. Clean the silicon wafer before spin-coating. Rinse a bare 2 inch silicon wafer with acetone for 15 min followed by isopropyl alcohol (IPA) for 15 min. Dehydrate the wafer by placing it on a hotplate at 150 °C for 1 hr. After dehydration, cool the wafer at room temperature.
    2. Spin-coat the silicon wafer with SU-8 photoresist. Add 2 ml SU-8 photoresist onto the wafer. Ramp the wafer to 500 rpm at 100 rpm/sec acceleration for 10 sec, followed by 1,000 rpm at 300 rpm/sec acceleration for 30 sec. (see Supplemental Video 1)
    3. Pre-bake the wafer on a hot plate at 65 °C for 10 min, then soft bake at 95 °C for 30 min.
    4. Use UV exposure to transform the designed pattern from a film mask to the spin-coated photoresist. Print the pattern on a thin transparent film as a film mask. Place the film mask on top of the spin-coated photoresist and expose to UV with a dose of 300 mJ/cm^2. (see Supplemental Video 2)
    Note: In this protocol, the microchannel network pattern (159 μm wide mother channels branching into four 100 μm wide daughter channels) is designed with CAD software. The pattern on the film shows as a clear field and the rest of the film is covered by black ink. Because SU-8 is a negative photoresist, the portion of the photoresist that is exposed to UV will be crosslinked and become insoluble to the solvent during the mold development (step 1.1.6). After the development, this insoluble portion will replicate the designed network pattern and serve as a master mold.
    5. Post-bake the exposed wafer on a hot plate at 65 °C for 1 min, then 95 °C for 10 min.
    6. Develop the master mold. Use SU-8 developer as the solvent to remove the un-crosslinked photoresist. Immerse the wafer in SU-8 developer for 3 min and rinse with IPA for 1 min.
    7. Repeat this developing cycle 2-3 times until there is no white streak formation (residue of non-cured photoresist) after the IPA rinse. Gently dry the wafer with nitrogen gas and examine the small features of the pattern under a microscope. Repeat additional developing cycles if necessary.
    8. Hard bake the wafer on a hot plate at 150 °C for 15 min.

2. Soft Lithography
    1. Manually mix the two parts (base and curing agent) of polydimethylsiloxane (PDMS) elastomer at a wt. ratio of 10:1.
    2. De-gas the PDMS mixture with a desiccator connected with a house vacuum for 15 min. Cast the PDMS solution on the photoresist master mold. The thickness of the PDMS needs to be over 3 mm to provide a stable holding of the inlet/outlet tubing. De-gas the PDMS again for 15 min, and remove the remaining air bubbles with nitrogen gas if necessary. Cure the casted PDMS in an oven at 65 °C for 3 hr.
    3. Clean the surface of the glass coverslip with a scotch tape and a plasma cleaner (30 sec plasma treatment). Spin-coat un-cured PDMS (0.5 ml) on the glass coverslip by ramping to 4,000 rpm at 500 rpm/sec acceleration rate for 30 sec. Cure the PDMS spin-coated coverslip in an oven at 65 °C for at least 30 min.
    4. Cut and release the cured PDMS from the master mold. Then create an inlet and an outlet with a 1 mm diameter hole puncher at the distal end of the mother channels.
    5. Bond the device to the PDMS spin-coated glass coverslip. Oxidize the surfaces of the PDMS and coverslip with a plasma cleaner for 1 min. After the oxygen plasma treatment, place a droplet of deionized water (DI water) at the bonding surface, and place the two parts together. Bake the device in an oven at 65 °C for 30 min to achieve a permanent bonding.

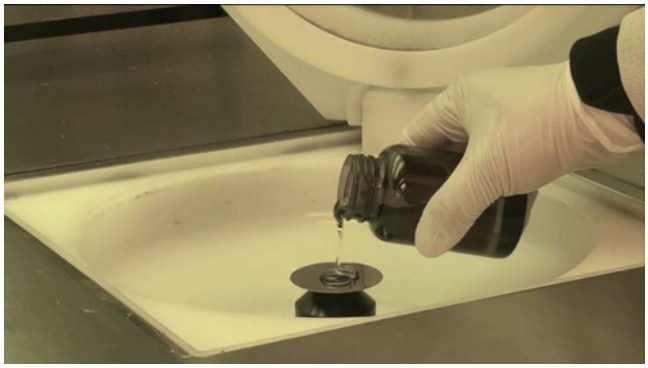

Supplemental Video 1 (Right click to download).

Supplemental Video 2 (Right click to download).

2. Endothelial Cell Seeding and Culture

1. Device Sterilization and Fibronectin Coating
    1. Preserve the hydrophobic property of the PDMS surface around the inlet/outlet from oxidation. Cover the PDMS surface around the inlet and outlet with small stripes of scotch tape to prevent oxidation. This procedure can prevent DI water from spreading all over the top surface of the device during the filling step (2.1.3).
    2. Treat the PDMS device with oxygen plasma for 5 min to change the surface to be hydrophilic, thus facilitate fluid flow through the microchannel and prevent the bubble trapping in the filling procedure (2.1.3).
    3. Use either a syringe with a needle attached or a pipette to fill the device with DI water from the inlet. Continue the filling until there is a droplet of DI water (30-50 µl) accumulated at the outlet. Examine the device under a microscope to check if there are bubbles trapped inside the microchannel. Remove the excessive water droplet at the inlet and outlet with a paper tissue.
    4. Sterilize the device in a petri dish with UV for a minimum of 3 hr in a laminar biosafety hood. To prevent evaporation, cover the inlet/outlet with a thin piece of PDMS, put a wet paper tissue inside the dish, and wrap the dish with Parafilm.
    5. Coat the device with fibronectin. Rinse the device first with phosphate-buffered saline (PBS), then coat it with 100 µg/ml fibronectin overnight in a refrigerator (4 °C). Place a droplet of solution at the inlet, and then create a negative pressure at the outlet with a house vacuum, a syringe with a needle or a pipette.
    6. Fill the device with cell culture media. Rinse the device with PBS manually for 3 times before loading the cell culture media. Warm up the device in an incubator at 37 °C.

2. ECs Seeding and Long-term Perfusion
   Note: Comparing with conventional static 2D EC culture, the *in vitro* microvessel network model with continuous perfusion made the cell culture environment closer to the *in vivo* conditions. The *in vitro* microvessel network demonstrated in this protocol can be maintained up to two weeks. The well-controlled perfusion will continuously replenish nutrients, remove wastes, and prevent over-confluence of the EC monolayer. Therefore, it can be extended to a longer term studies, mimicking the cellular and hemodynamic environment under different physiological and pathological conditions.
    1. Mix primary HUVECs in HUVEC culture media (MCDB 131) with 8% dextran (mol wt 70,000). The dextran is used to increase the viscosity of the loading media and achieve a better cell seeding result. The recommended cell density is about 2-4 x 10^6 cells/ml.
    2. Seed the cells into the device. Place a 10-20 µl droplet of cells over the inlet. Introduce a gentle flow by either tilting the device, or capillary action using a glass Pasteur pipette at the outlet. The key for a successful cell loading is to control the flow velocity less than 1 mm/sec within the smallest channels.
    3. Check the cell seeding. After the initial seeding, incubate the device for 15-20 min (humidified atmosphere of 5% CO_2 at 37 °C) before checking the seeding status under the microscope. If necessary, perform additional cell loading to achieve a desired cell density.
    4. Gently rinse the device with cell culture medium (37 °C) to remove the dextran. Culture the device in the absence of flow for the first 6 hr in an incubator (5% CO_2 at 37 °C).
    5. Set up the tubing connection for long-term perfusion. Tape the device into a petri dish to prevent movement. Create small holes on the lid of the Petri dish for inlet and outlet tubing insertions. Connect the inlet tubing to a syringe with a needle for the cell culture media perfusion. Connect the outlet tubing to a waste collector.

Note: Place the device and the waste collector in a cell culture incubator, while placing a perfusion pump outside of the incubator and connect it with the device by the long inlet tubing. The perfusion rate is determined by the experimental design. In the present device, use a perfusion rate of 0.35 µl/min and a shear stress range between 1-2 dyne/cm^2. Under this perfusion condition, the HUVECs reach confluence in about 3-4 days.

3. Immunofluorescent Staining

1. Fix the ECs in the device by perfusion of 2% paraformaldehyde for 30 min at 4 °C, followed by 1x PBS rinsing at room temperature for 15 min, and 1% BSA blocking for 30 min. Use a perfusion rate that is the same as that used for cell culture.
2. Permeabilize the fixed ECs for antibody staining with 0.1% Triton X-100. Perfuse the device with Triton for 5-7 min to label VE-cadherin, and 3 min to label F-actin.
3. Load the antibodies into the device. Perfuse the device with 1x PBS for 15 min to wash out the previous solutions. Manually load the primary antibody against VE-cadherin (anti-goat) into the device at the concentration of 2 µg/ml (the total volume is 20-50 µl). Keep the device in a refrigerator at 4 °C overnight. Perfuse the secondary antibody (donkey anti-goat) by a syringe pump at the concentration of 7 µg/ml for 45-60 min.
4. Label EC F-actin with phalloidin. Perfuse the device with 1x PBS for 15 min before manually loading phalloidin (10 µg/ml) for 7-10 min.
5. Label EC nuclei (see Materials List).
6. Rinse the device with 1x PBS, and maintain it at 4 °C until imaging.

4. Fluorescence Imaging of Endothelial $[Ca^{2+}]_i$

1. Perfuse the device with albumin (10 mg/ml)-Ringer's solution for 15 min at 37 °C. Use the same perfusion rate as that used for cell culture. The concentrations of all components of albumin-Ringer's solution are described in the **Materials List**.
2. Set up confocal system for EC $[Ca^{2+}]_i$ imaging with fluo-4 AM. Use a confocal microscopic system for Ca^{2+} imaging. Use an argon laser (488 nm) for excitation and set the emission band as 510-530 nm. Collect the images with a 25X objective (water immersion, NA: 0.95) at 512 x 512 scan format. Use a z-step of 2 µm and a scanning interval for each stack of images of 20 sec.
3. Perfuse the device with fluo-4 AM (5 µM) for 40 min at 37 °C, then wash out the lumen fluo-4 AM with albumin-Ringer's solution.
4. Acquire images of fluo-4 loaded microvessels. Collect the baseline images for 10 min. Perfuse the device with ATP (10 µM) and record the changes of fluorescence intensity (FI) for 20 min.

5. Fluorescence Imaging of Nitric Oxide Production

1. Perfuse the device with albumin-Ringer's solution for 15 min. Use a perfusion rate that is the same as that used for cell culture.
2. Set up the fluorescence imaging system to measure ATP-induced nitric oxide production. Use a microscope equipped with a 12-bit digital CCD camera and a computer-controlled shutter for nitric oxide measurement. Use a 75 W xenon lamp as the light source.
   Note: Select the excitation and emission wavelength for DAF-2 DA by an interference filter (480/40 nm) and a dichroic mirror (505 nm) with a band-pass barrier (535/50 nm). Use a 20X objective lens (NA: 0.75) to collect the images. To minimize photobleaching, position a neutral density filter (0.5 N) in front of the interference filter and limit the exposure time to 0.12 sec.
3. Load the cells with DAF-2 DA (5 µM). Perfuse the device with DAF-2 DA for about 35-40 min at 37 °C. Record the baseline of DAF-2 fluorescence intensity (FI_{DAF}) after the initial loading.
   Note: DAF-2 DA is continuously present in the perfusate throughout the experiment[7].
4. Collect DAF-2 images. Record the baseline of FI_{DAF} for 5 min. Perfuse the device with ATP (10 µM) and collect the images for 30 min with 1 min intervals. Collect all of the images from the same group of cells at the same focal plane.

6. Data Analysis

1. Manually select the region of interests (ROIs) from the collected images at individual cell level. Each ROI covers the area of one individual cell which can be indicated by the fluorescence outline.
2. Subtract background fluorescence and calculate the mean FI of each ROIs.
3. Measure ATP-induced changes in EC $[Ca^{2+}]_i$ and NO production. Quantify ATP-induced changes in EC $[Ca^{2+}]_i$ by calculating the changes in Fluo-4 FI (FI/FI_0*100, where FI_0 is the average baseline FI during albumin-Ringer perfusion before adding ATP) minus the measured background. Quantify NO production rate by conducting the first differential conversion of the FI_{DAF} over time.
   Note: The time course of FI_{DAF} represents a cumulative NO production with time. Therefore, NO production rate is calculated based on the profile of FI_{DAF} under both basal and ATP stimulated conditions. Details of data analysis and experimental procedures have been described in a previous publication[7].

Representative Results

This section shows some of the results obtained with the cultured microvessel network developed with this protocol. The microchannel pattern is a three level branching network (**Figure 1A**). In this design, a 159 µm wide mother channel branches into two 126 µm wide channels, and branches again into four 100 µm wide daughter channels. A 3D numerical simulation was performed to estimate the shear stress distributions under the flow rate of 0.35 µl/min (**Figure 1B**), which indicates three different levels of shear stress within this microchannel network. The laminar flow within the microchannels is predicted to be hydrodynamically stable without the presence of disturbed or secondary flow. After a SU-8 master mold was fabricated with a standard photolithography process (**Figure 1C**), a PDMS device was fabricated through soft lithography to replicate the microchannel network design into a transparent, air permeable scaffold (**Figure 1D**-**E**). After EC seeding (**Figure 1F**-**G**) and 3-4 days of continuous perfusion, ECs reached confluence and successfully covered the inner surfaces of the microchannels.

EC F-actin and nuclei were fluorescently labeled within the network and illustrated with confocal images. Under the shear stress of 1.0 dyne/cm^2, about 30% of the HUVECs elongated along the flow direction with increased central stress fibers, whereas the rest 70% maintained its cobblestone pattern with dominated peripheral F-actin[5]. The shear-induced cell shape change appears less prominent than that commonly observed in 2D static cell cultures. Actually under *in vivo* conditions, the ECs have different cell shapes in different types of vessels, but not easily change cell shape in response to the flow changes. More studies are needed to determine whether this difference was the results of the channel geometry and perfusion environment that are closer to *in vivo* conditions.

We also successfully measured ATP-induced changes in EC $[Ca^{2+}]_i$ and NO production (**Figures 4** and **5**). ATP induced transient increases in EC $[Ca^{2+}]_i$ and NO production. The mean peak FI_{fluo-4} was 187 ± 22% of the baseline, which occurred at 35 ± 10 sec after the start of ATP perfusion. The NO production rate was increased from a basal level of 0.15 ± 0.05 AU per min to 1.18 ± 0.37 AU per min within the first five minutes of ATP exposure. All the results were reported as the mean ± standard error (SE). They are comparable to the results derived from individually perfused intact venules[6,9,14,19].

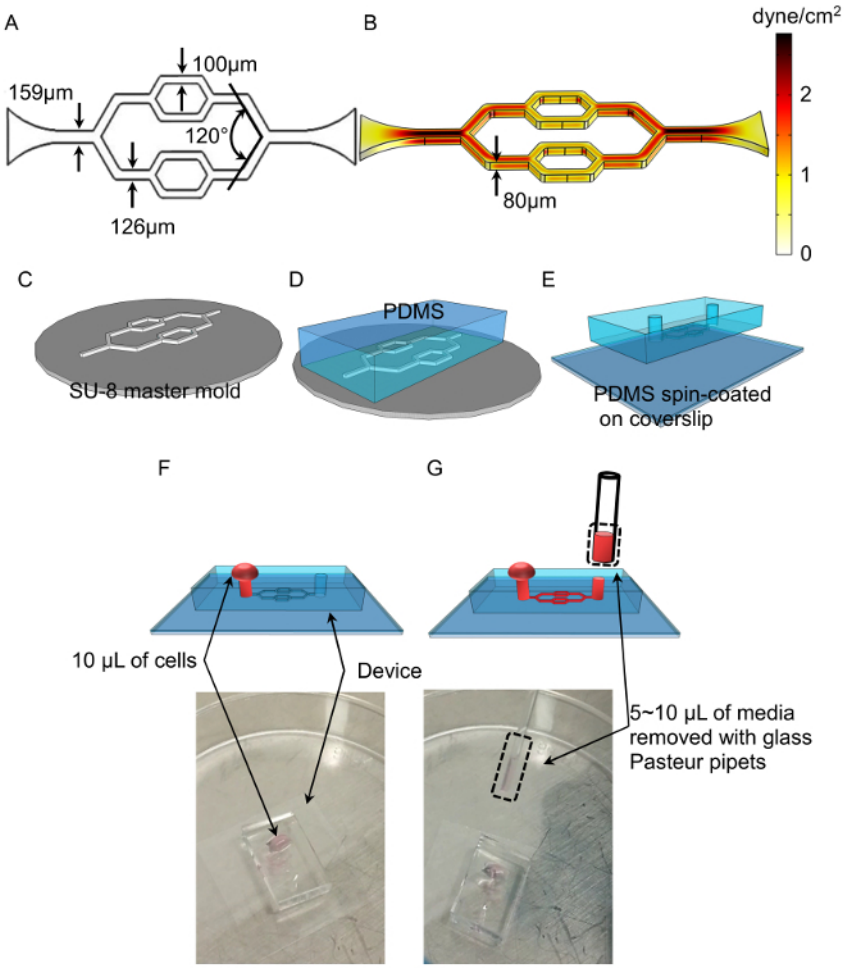

Figure 1: Microfluidic Device Fabrication and EC loading. (**A**) The schematic view of the microchannel network. The width and bifurcation angle of the microchannels are indicated at each branching levels. (**B**) The numerical simulation of shear stress distribution. The flow rate is 0.35 μl/min. The height of the microchannel after development is 80 μm. These two figures have been modified from previous publication with additional details[5]. (**C**) The development of the master mold. The master mold of the microchannel network is fabricated with SU-8 photoresist on silicon wafer. (**D**) The process of soft lithography. PDMS mixture is casted onto the master mold and cured in an oven. (**E**) Bonding PDMS channel to the substrate. The substrate used for this device is a coverslip spin coated with a thin layer of PDMS. The inlet and outlet are created with a hole-puncher. (**F** and **G**) EC loading. About 10 μl of cell solution is placed at the inlet. A gentle flow is then induced by placing a Pasteur pipette at the outlet via capillary flow. Please click here to view a larger version of this figure.

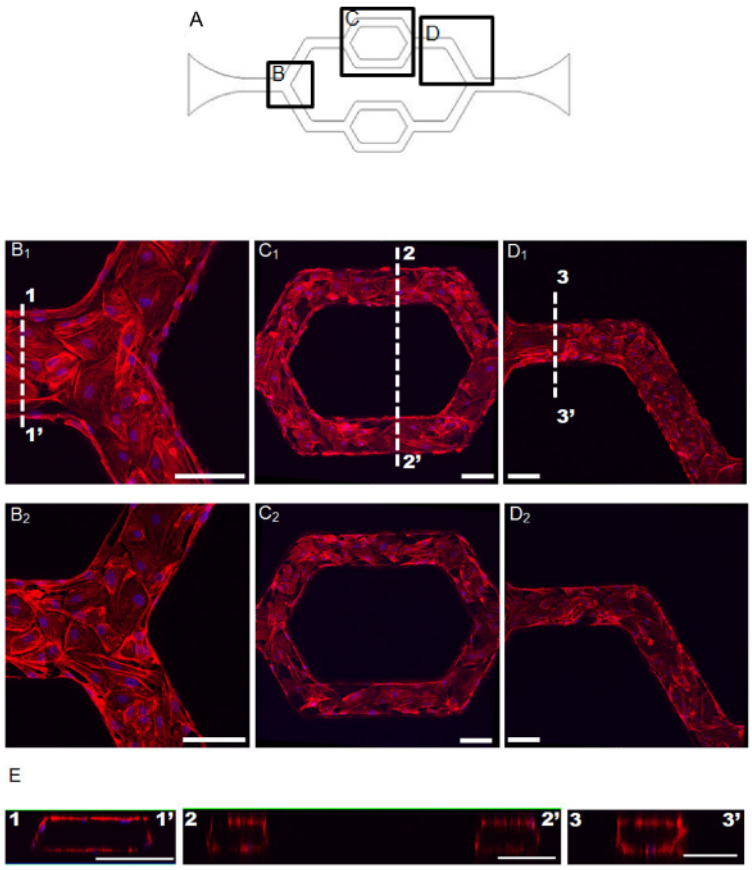

Figure 2: Confocal images of EC F-actin in cultured microchannel network. (**A**) A schematic view of the network design. The selected regions shown in **B**-**D** are indicated in the graph. (**B**-**D**) Confocal images of EC F-actin (red) and nuclei (blue) of the *in vitro* microvessel network. **B_1**, **C_1** and **D_1** are the projected images from top half of the microchannel image stacks, and **B_2**, **C_2**, and **D_2** are the image projections from lower half of the image stacks. E. The cross-sectional view indicated as 1-1', 2-2', and 3-3' in **B_1**-**D_1**, Scale bar = 100 µm. These images are adapted from previous publication[5]. Please click here to view a larger version of this figure.

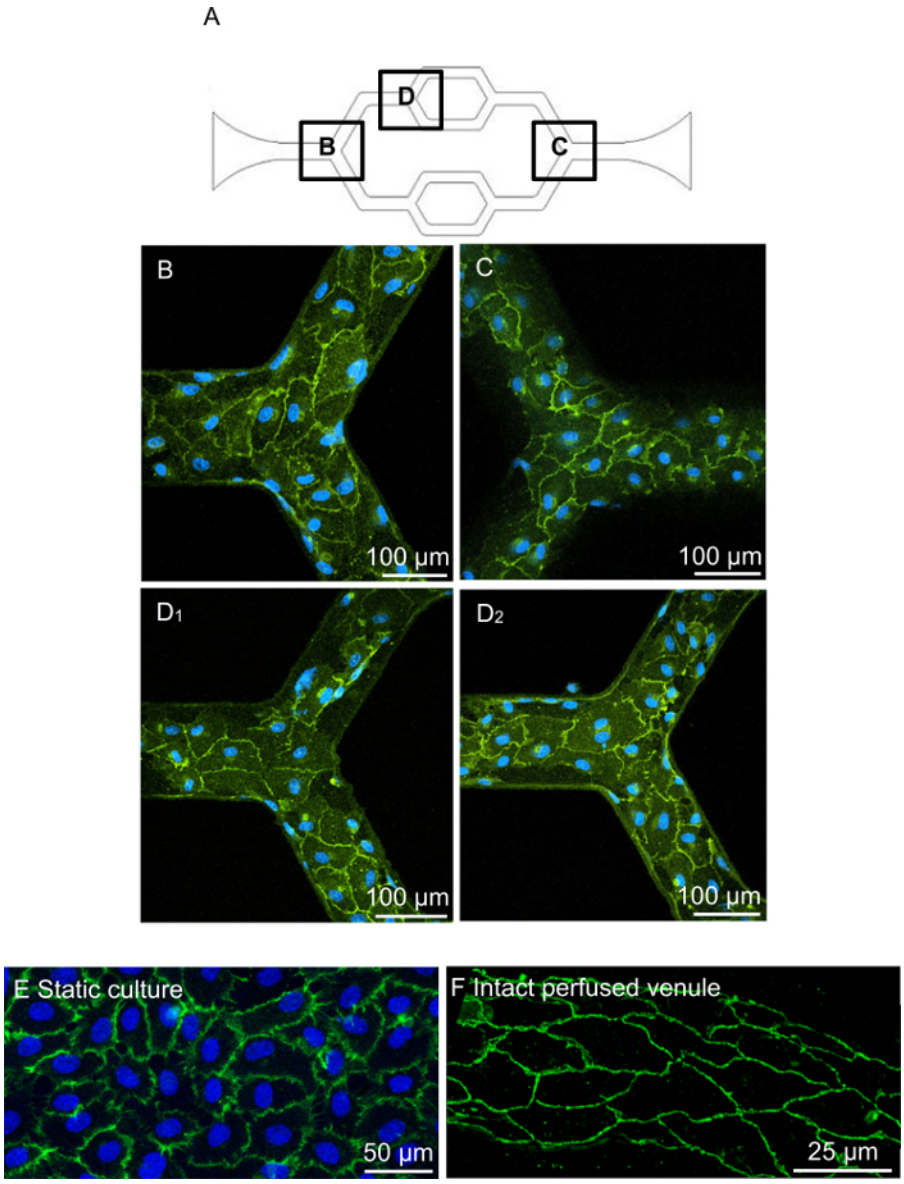

Figure 3: Comparisons of VE-cadherin distribution in cultured microvessel network with statically cultured EC monolayer and intact rat mesenteric venule. (**A**) The schematic view of the network design with selected regions shown in **B**-**D**. (**B**-**D**) VE-cadherin (green) and cell nuclei (blue) staining of the *in vitro* microvessel network. $\mathbf{D_1}$ and $\mathbf{D_2}$ are the top and bottom of the projected images collected from the same bifurcation region, respectively. (**E**) VE-cadherin staining of statically cultured ECs. (**F**) VE-cadherin staining of individually perfused intact rat venule. This figure published previously[5]. Please click here to view a larger version of this figure.

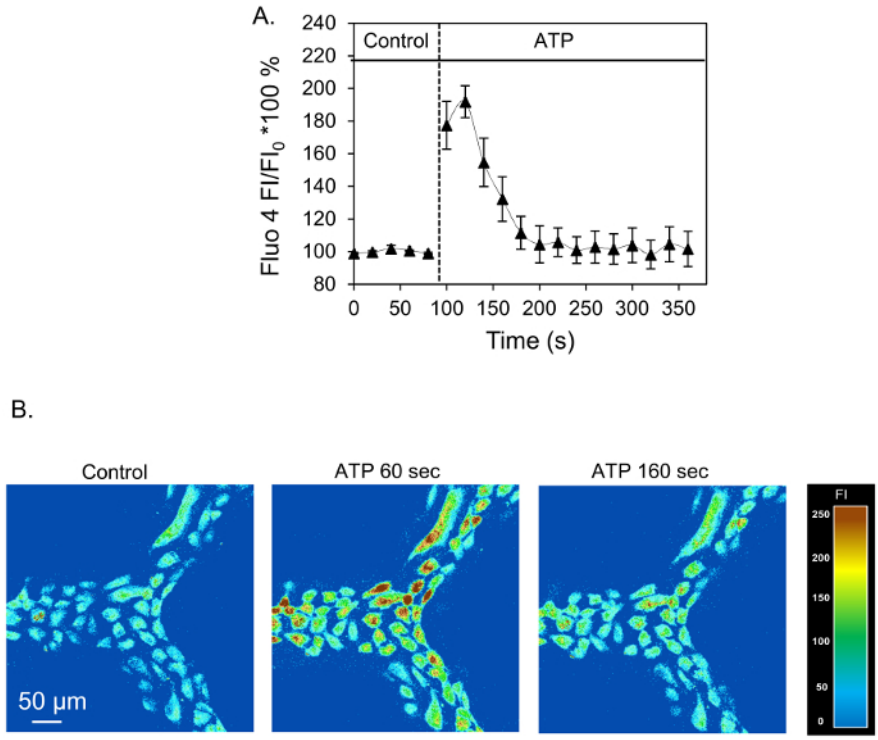

Figure 4: ATP-induced increases in EC $[Ca^{2+}]_i$. Experiments were conducted from 4 devices and 7 to 12 ROIs (individual ECs) per device were selected for data analysis. (**A**) The time course of ATP (10 µM)-induced changes in EC $[Ca^{2+}]_i$ (Fluo 4 FI/FI_0×100% ± SE) from one representative experiment. (**B**) The images of the representative experiment (data is shown in A). This is a previously published figure[5]. Please click here to view a larger version of this figure.

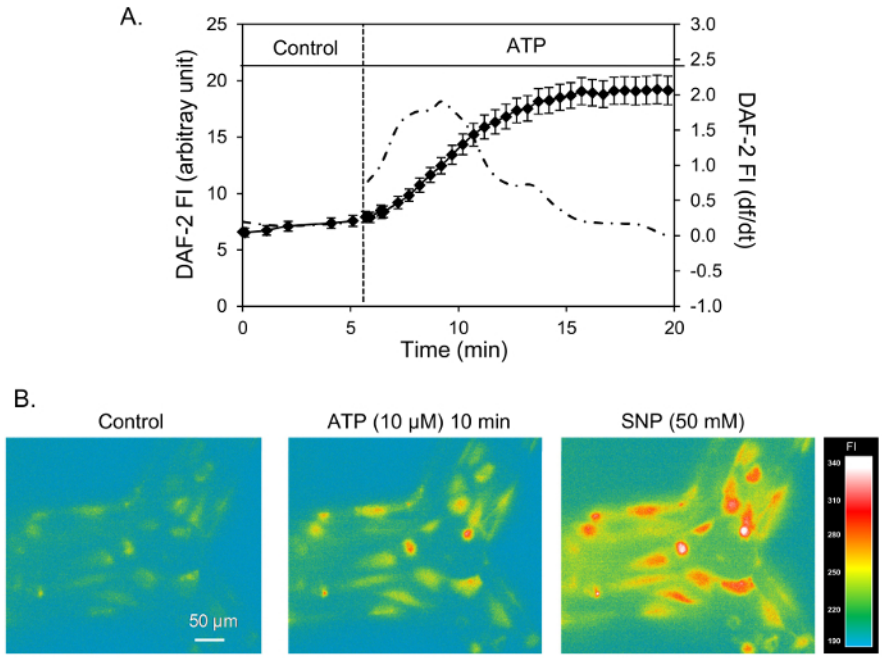

Figure 5: ATP-induced NO production. Experiments were conducted in 3 devices and 11 to 12 ROIs (individual ECs) per device were selected for data analysis. (**A**) Time dependent changes of DAF-2 fluorescence intensity (FI_{DAF} ± SE, left Y axis) in ECs under basal conditions and after exposure to ATP. The NO production rate (df/dt, dotted line), was derived from the first differential conversion of the accumulated FI_{DAF} (right Y axis). (**B**) Representative images from one experiment. The FI_{DAF} further increased after a NO donor, sodium nitroprusside (SNP), was added to the perfusate, indicating a sufficient amount of intracellular DAF-2 to react with NO. This is a previously published figure[5]. Please click here to view a larger version of this figure.

Discussion

In this article, we present detailed protocols for the development of cultured microvessel network, the characterization of EC junctions and cytoskeleton F-actin distribution, and the quantitative measurements of EC $[Ca^{2+}]_i$ and NO production using a microfluidic device. The perfused microfluidic device provides an *in vitro* model that allows a close simulation of the *in vivo* microvascular geometries and shear flow conditions. Since the cultured microvessel network can be formed by primary human ECs, this approach can serve as a useful tool to investigate how pathologically altered blood components from patient samples affect human ECs by direct perfusion of patient blood samples to the cultured microvessels and provide insight into clinical issues. The human ECs developed microvessels can also be used for drug screening to avoid the potential discrepancies in drug responses between human and animal tissues.

The substrate of the microfluidic devices shown in this protocol is a glass cover-slip (150-180 μm) spin-coated with a thin layer of PDMS. This thin layer of PDMS is essential for high resolution and live tissue real time imaging, because the larger numerical aperture objectives usually has short working distance. The laminar flow within the microchannel (submillimeter range) has a very low Reynolds number, and the pressure differential is linearly related to the flow, thus the shear stress distribution is solely dependent on the channel geometry. Therefore, it can be well-controlled by high-accuracy perfusion pump[20]. In our present study, the shear stress applied to the HUVEC cultured microvessel network was between 1 to 10 dyne/cm^2, which is within the range of shear stress measured in the venous system[21,22]. The macro-fluidic systems such as parallel flow chamber lacks complex flow patterns. In larger scale flow chambers (mm-cm range), ECs are typically only grown in the bottom surface (2D monolayer), lacking the geometric similarities to microvessels *in vivo*. When the width of the flow chamber is over 2 mm, the homogeneous flow is confined in a region that is usually several millimeters away from the outlet/inlet, and a couple hundred microns away from the side wall[23]. When the width of the chamber is increased to the range of centimeters, the flow will differentiate into various streamlines and the flow velocities will change across the whole area[24]. Additionally, the larger scale flow chamber consumes at least 100 times more perfusate to achieve the same shear stress as that in microchannels. The shear stress distribution within the microchannel network can be simulated using a numerical modeling tool, and the stationary incompressible Navier-Stokes equations can be solved by most finite element software.

The microfluidic device can be made with a single mask microfabrication process. The success of cultured microvessel development, however, requires special attentions to the details. After loading the solution into the microchannels, each device needs to be checked for bubble trapping under the microscope before EC seeding. If a bubble occurs, it is still possible to force it out at this stage by applying a hydraulic pressure at the inlet with a closed outlet, as PDMS is an air-permeable material. To maintain a desired perfusion rate, tight fitting without a leak is necessary for all of the needle/tubing connections. The matched hole-puncher and tubing size are critical to achieve a tight fitting. To assure a precise delivery of the flow rate, the syringe on the perfusion pump and the device should be placed at the same level. To change the perfusate, the inserted tubing should be gently disconnected from the device to avoid any stretching. To increase shear stress, step increases (such as 10 steps of increase in 18 hr) are recommended to avoid sudden flow change caused EC peeling.

Previous studies performed on individually perfused intact microvessels indicated that agonist-induced increases in EC $[Ca^{2+}]_i$, and the subsequent endothelial nitric oxide synthase (eNOS) activation and NO production are necessary signaling for increased microvascular permeability under inflammatory conditions[6,7,9-13,25]. In this protocol, we select ATP as the representative agonist, since it is commonly released by red blood cells, aggregated platelets, and injured tissues or under inflammatory conditions *in vivo*. A fluorescence calcium indicator, Fluo-4 AM, was used to measure the changes in endothelial $[Ca^{2+}]_i$ after exposure to ATP. The EC $[Ca^{2+}]_i$ responses in cultured microvessels are similar to those found in intact microvessels[7,9]. Measuring EC NO production has been technically challenging for biologists. To date, there has been no fluorescent indicator that enables the detection of dynamic changes in NO concentration in a similar manner to the calcium indicators. DAF-2 DA has been widely used to assess NO production. However, the proper usage, data interpretation, and data analysis need to draw users' attention. Since the chemical transformation of DAF-2 to DAF-2T in the presence of NO is irreversible (one way conversion)[26], the detected DAF fluorescence intensity profile does not represent the changes in NO concentration. Instead, it indicates the accumulated DAF-2T production with time. Based on this cumulated DAF-2 fluorescence (FI_{DAF}) curve, the NO production rate (df/dt) can be derived by the first differential conversion of the FI_{DAF}[7,11]. Namely, the slope of the FI curve indicates the NO production rate and the plateau phase indicates no further increased NO production. After the conversion, the data generated from this protocol presented both the basal NO production rate and the changes in NO production in response to ATP with temporal and spatial resolution at individual EC levels within the microvessel network.

Currently PDMS has been widely used for microfluidic applications, as it is an optically transparent, nontoxic, and gas permeable soft elastomer[27-30]. However, since PDMS is not water permeable, we could not directly measure the permeability of EC monolayer. To overcome this limitation, some applications modified the channel wall structures such as integrating a permeable membrane into the channel[31], or creating a permeable "window openings" with micro-pillars or micro-holes[32,33], while others have been focused on the modification of device materials such as using the hydrogel devices or hydrogel/PDMS hybrid devices[17,34-36]. The drawbacks of such devices are their vulnerable nature to dehydration and their relatively weak mechanical properties to stand stress or pressure. Future development of permeable material with mechanical strength will further improve the device and its potential for broader biological applications.

Disclosures

The authors have no competing interests or conflicting interests to disclose.

Acknowledgements

This work was supported by National Heart, Lung, and Blood Institute grants HL56237, National Institute of Diabetes and Digestive and Kidney Diseases Institute DK97391-03, National Science Foundation (NSF-1227359 and EPS-1003907).

References

1. Curry, F. R. E., & Adamson, R. H. Vascular permeability modulation at the cell, microvessel, or whole organ level: towards closing gaps in our knowledge. *Cardiovasc Res.* **87**, 218-229 (2010).
2. Michel, C. C., & Curry, F. E. Microvascular permeability. *Physiol Rev.* **79**, 703-761 (1999).
3. Rogers, J. A., & Nuzzo, R. G. Recent progress in soft lithography. *Mater Today.* **8**, 50-56 (2005).
4. Sackmann, E. K., Fulton, A. L., & Beebe, D. J. The present and future role of microfluidics in biomedical research. *Nature.* **507**, 181-189 (2014).
5. Li, X., Xu, S., He, P., & Liu, Y. In vitro recapitulation of functional microvessels for the study of endothelial shear response, nitric oxide and [Ca^{2+}]I. *PLoS One.* **10**, e0126797 (2015).
6. He, P., Pagakis, S. N., & Curry, F. E. Measurement of cytoplasmic calcium in single microvessels with increased permeability. *Am J Physiol.* **258**, H1366-1374 (1990).
7. Zhou, X., & He, P. Improved measurements of intracellular nitric oxide in intact microvessels using 4,5-diaminofluorescein diacetate. *Am J Physiol-Heart C.* **301**, H108-H114 (2011).
8. Yuan, D., & He, P. Vascular remodeling alters adhesion protein and cytoskeleton reactions to inflammatory stimuli resulting in enhanced permeability increases in rat venules. *Journal of Applied Physiology.* **113**, 1110-1120 (2012).
9. He, P., Zhang, X., & Curry, F. E. Ca2+ entry through conductive pathway modulates receptor-mediated increase in microvessel permeability. *Am J Physiol.* **271**, H2377-2387 (1996).
10. Zhou, X., & He, P. Endothelial [Ca2+]i and caveolin-1 antagonistically regulate eNOS activity and microvessel permeability in rat venules. *Cardiovasc Res.* **87**, 340-347 (2010).
11. Zhu, L., & He, P. Platelet-activating factor increases endothelial [Ca2+] i and NO production in individually perfused intact microvessels. *Am J Physiol-Heart C.* **288**, H2869-H2877 (2005).
12. He, P., & Curry, F. E. Depolarization modulates endothelial cell calcium influx and microvessel permeability. *Am J Physiol.* **261**, H1246-1254 (1991).
13. He, P., & Curry, F. E. Endothelial cell hyperpolarization increases [Ca2+]i and venular microvessel permeability. *J Appl Physiol (1985).* **76**, 2288-2297 (1994).
14. Xu, S., Zhou, X., Yuan, D., Xu, Y., & He, P. Caveolin-1 scaffolding domain promotes leukocyte adhesion by reduced basal endothelial nitric oxide-mediated ICAM-1 phosphorylation in rat mesenteric venules. *Am J Physiol Heart Circ Physiol.* **305**, H1484-1493 (2013).
15. Zadeh, M. H., Glass, C. A., Magnussen, A., Hancox, J. C., & Bates, D. O. VEGF-Mediated Elevated Intracellular Calcium and Angiogenesis in Human Microvascular Endothelial Cells In Vitro are Inhibited by Dominant Negative TRPC6. *Microcirculation.* **15**, 605-614 (2008).
16. Tsai, M. *et al.* In vitro modeling of the microvascular occlusion and thrombosis that occur in hematologic diseases using microfluidic technology. *The Journal of clinical investigation.* **122**, 408-418 (2012).
17. Kim, S., Lee, H., Chung, M., & Jeon, N. L. Engineering of functional, perfusable 3D microvascular networks on a chip. *Lab Chip.* **13**, 1489-1500 (2013).
18. Amico Oblak, T., Root, P., & Spence, D. M. Fluorescence monitoring of ATP-stimulated, endothelium-derived nitric oxide production in channels of a poly(dimethylsiloxane)-based microfluidic device. *Analytical chemistry.* **78**, 3193-3197 (2006).
19. Zhou, X. P., Yuan, D., Wang, M. X., & He, P. N. H2O2-induced endothelial NO production contributes to vascular cell apoptosis and increased permeability in rat venules. *Am J Physiol-Heart C.* **304**, H82-H93 (2013).
20. Lee, P. J., Hung, P. J., Rao, V. M., & Lee, L. P. Nanoliter scale microbioreactor array for quantitative cell biology. *Biotechnol Bioeng.* **94**, 5-14 (2006).
21. Zakrzewicz, A., Secomb, T. W., & Pries, A. R. Angioadaptation: Keeping the Vascular System in Shape. *Physiology.* **17**, 197-201 (2002).
22. Lipowsky, H. H., Kovalcheck, S., & Zweifach, B. W. The distribution of blood rheological parameters in the microvasculature of cat mesentery. *Circulation Research.* **43**, 738-749 (1978).
23. Pisano, M., Triacca, V., Barbee, K. A., & Swartz, M. A. An in vitro model of the tumor-lymphatic microenvironment with simultaneous transendothelial and luminal flows reveals mechanisms of flow enhanced invasion. *Integr Biol (Camb).* **7**, 525-533 (2015).
24. McCann, J. A., Peterson, S. D., Plesniak, M. W., Webster, T. J., & Haberstroh, K. M. Non-uniform flow behavior in a parallel plate flow chamber : alters endothelial cell responses. *Ann Biomed Eng.* **33**, 328-336 (2005).
25. Curry, F. E. Modulation of venular microvessel permeability by calcium influx into endothelial cells. *FASEB J.* **6**, 2456-2466 (1992).
26. Kojima, H. *et al.* Detection and imaging of nitric oxide with novel fluorescent indicators: diaminofluoresceins. *Anal Chem.* **70**, 2446-2453 (1998).
27. Whitesides, G. M. The origins and the future of microfluidics. *Nature.* **442**, 368-373 (2006).
28. Lamberti, G. *et al.* Bioinspired microfluidic assay for in vitro modeling of leukocyte-endothelium interactions. *Anal Chem.* **86**, 8344-8351 (2014).
29. Myers, D. R. *et al.* Endothelialized microfluidics for studying microvascular interactions in hematologic diseases. *J Vis Exp.* (2012).
30. Smith, A. M., Prabhakarpandian, B., & Pant, K. Generation of Shear Adhesion Map Using SynVivo Synthetic Microvascular Networks. *Jove-J Vis Exp.* e51025 (2014).
31. Booth, R., & Kim, H. Characterization of a microfluidic in vitro model of the blood-brain barrier (iBBB) (vol 12, pg 1784, 2012). *Lab on a Chip.* **12**, 5282-5282 (2012).
32. Shao, J. B. *et al.* Integrated microfluidic chip for endothelial cells culture and analysis exposed to a pulsatile and oscillatory shear stress. *Lab on a Chip.* **9**, 3118-3125 (2009).
33. Yeon, J. H. *et al.* Reliable permeability assay system in a microfluidic device mimicking cerebral vasculatures. *Biomed Microdevices.* **14**, 1141-1148 (2012).
34. Golden, A. P., & Tien, J. Fabrication of microfluidic hydrogels using molded gelatin as a sacrificial element. *Lab Chip.* **7**, 720-725 (2007).
35. Zheng, Y. *et al.* In vitro microvessels for the study of angiogenesis and thrombosis. *Proc Natl Acad Sci U S A.* **109**, 9342-9347 (2012).
36. Baker, B. M., Trappmann, B., Stapleton, S. C., Toro, E., & Chen, C. S. Microfluidics embedded within extracellular matrix to define vascular architectures and pattern diffusive gradients. *Lab Chip.* **13**, 3246-3252 (2013).

